

1           **STICr: An open-source package and workflow for Stream Temperature,**  
2                           **Intermittency, and Conductivity (STIC) data**

3  
4 **Authors:** Sam Zipper<sup>a,b,\*</sup>, Christopher T. Wheeler<sup>a,b</sup>, Delaney M. Peterson<sup>c</sup>, Stephen C. Cook<sup>d</sup>,  
5 Sarah E. Godsey<sup>e</sup>, Ken Aho<sup>e</sup>

6  
7 **Affiliations:**

8 <sup>a</sup>Kansas Geological Survey, University of Kansas, Lawrence KS

9 <sup>b</sup>Department of Geology, University of Kansas, Lawrence KS

10 <sup>c</sup>Department of Biological Sciences, University of Alabama, Tuscaloosa AL

11 <sup>d</sup>Department of Biology, University of Oklahoma, Norman, OK

12 <sup>e</sup>Department of Geosciences, Idaho State University, Pocatello, ID

13 \* Corresponding author: Sam Zipper ([samzipper@ku.edu](mailto:samzipper@ku.edu))

14  
15 **ORCID IDs:**

16 Zipper: 0000-0002-8735-5757

17 Wheeler: 0000-0001-9368-383X

18 Cook: 0000-0003-3642-1790

19 Peterson: 0000-0002-3444-4772

20 Godsey: 0000-0001-6529-7886

21 Aho: 0000-0001-5998-2916

22  
23 **Highlights:**

- 24       • Stream intermittency datalogger output requires substantial processing  
25       • The STICr R package provides functions to process, analyze, and QAQC this data  
26       • We share a project-wide workflow for creating FAIR stream intermittency data  
27       • In Kansas, STIC data reveal spatial stream intermittency response to geology  
28       • Temporal stream intermittency linked to precipitation and ET at different time lags

29 **Keywords:** hydrology, R, non-perennial streams, stream intermittency, Konza Prairie, FAIR  
30 data, groundwater

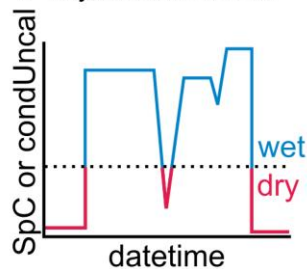
31  
32 *Draft manuscript submitted to Environmental Modeling & Software for peer review*  
33

34 **Abstract**

35 Non-perennial streams constitute over half the world’s stream miles but are not commonly  
36 included in national streamflow monitoring networks. Stream Temperature, Intermittency, and  
37 Conductivity (STIC) loggers are a widely used tool for studying non-perennial streams because  
38 they provide a relatively inexpensive and robust method for characterizing flow presence or  
39 absence. However, raw data downloaded from STIC loggers must be processed to generate  
40 hydrologically-meaningful data including temperature, conductivity, and interpreted  
41 classification of “wet” or “dry” readings at each timestep. To facilitate ‘FAIR’ (findable,  
42 accessible, interoperable, and reusable) stream intermittency science, we present an open-source  
43 package, STICr, written in the R language to provide a standardized framework for processing  
44 data from STIC loggers. STICr includes functions to tidy data, develop and apply sensor  
45 calibrations, classify data into wet/dry readings, and perform quality checks and validation on  
46 classified data. We also show a reproducible project-wide data workflow based on STICr for  
47 organizing and processing data from over 200 STIC loggers spanning multiple watersheds, years,  
48 and research groups, highlighting how interdisciplinary project considerations drive data  
49 processing considerations. Using South Fork Kings Creek (Konza Prairie, Kansas, USA) as a  
50 case study, we use STICr-processed data to identify spatial and temporal drivers of stream  
51 intermittency. For this watershed, stream intermittency is driven by the balance between monthly  
52 precipitation inputs and seasonal evapotranspiration fluxes, with spatial patterns of flow  
53 durations driven by underlying geology. This demonstrates how STICr can be used to create  
54 FAIR stream intermittency data and enable advances in hydrologic and ecosystem science.

56 **Graphical Abstract**

**STICr:** Tools for processing Stream Temperature, Intermittency, and Conductivity (STIC) sensors including tidying, calibration, classification, QAQC, and validation  
*STIC data collection* → *Tidy, classified data* → *Validation against field data*



		Classified	
		wet	dry
Observed	wet	25	5
	dry	3	21

57

## 58 1. Introduction

59 Non-perennial streams represent the majority of flowing water bodies worldwide  
60 (Messenger et al., 2021), and their prevalence in many regions has increased over the past four  
61 decades (Sauquet et al., 2021; Trambly et al., 2021; Zipper et al., 2021). Locally, the timing and  
62 spatial distribution of flow in non-perennial streams influences various ecosystem services  
63 (Kaletová et al., 2019; Stubbington et al., 2020), including carbon and nitrogen cycling (Aho et  
64 al., 2023; Hale and Godsey, 2019), biological community assemblages (Busch et al., 2024),  
65 ecosystem connectivity (Malish et al., 2024), and groundwater recharge (Shanafield and Cook,  
66 2014; Zipper et al., 2022). At regional scales, non-perennial streamflow dynamics ultimately  
67 influence the quantity and quality of water available for downstream users (Brinkerhoff et al.,  
68 2024). To support effective watershed management, accurate and high-resolution *in-situ*  
69 measurements of flow intermittence are needed to quantify the hydrologic controls on  
70 connectivity and characterize impacts on water quality and society (Shanafield et al., 2020a;  
71 Zimmer et al., 2022).

72 However, non-perennial streams are underrepresented in global stream monitoring  
73 networks (Krabbenhoft et al., 2022). To monitor non-perennial flow dynamics, Stream  
74 Temperature, Intermittency, and Conductivity (STIC) loggers are a low-cost and rapidly  
75 deployable tool. STICs are created by repurposing the circuitry used for recording light intensity  
76 in the widely-available Onset HOBO Pendant temperature and light data logger (model UA-002-  
77 64) to provide a relative measurement of electrical conductivity using two external electrodes  
78 (Chapin et al., 2014). Since electrical conductivity of water is substantially higher than that of  
79 air, conductivity recorded by STIC sensors can be interpreted and classified to produce a binary  
80 record of water presence or absence. Recently, additional intermittency sensors such as the Smart  
81 Rock (Milford and Truong, 2024) have been developed with similar functionality to STIC  
82 loggers.

83 Leveraging data from site-specific studies of stream intermittency into regional to global  
84 understanding requires developing findable, accessible, interoperable, and reusable (FAIR;  
85 Wilkinson et al., 2016) data on stream intermittency. However, while the field of hydrology has  
86 made efforts towards improved open science practices (Hall et al., 2022; Zipper et al., 2019), the  
87 discipline has been lagging with respect to FAIR data and computational resources (Reinecke et  
88 al., 2022; Stagge et al., 2019). Raw data from STICs and other sensors requires substantial  
89 processing to develop a FAIR time series of stream intermittency. Thus, there is a need for an  
90 open, standardized, and reproducible workflow for tidying STIC data and performing basic  
91 processing operations such as calibrating measured conductivity, generating the classified  
92 wet/dry dataset, and performing quality assurance and quality control (QAQC) checks on the  
93 data.

94 To advance these goals, we present a new open-source software package (STICr) for  
95 tidying and processing STIC logger data. While many R packages exist for working with sensor  
96 data, most were developed for specific sensor types (i.e., TDPanalysis for sap flow sensors,  
97 Durand, 2020; thermocouple for temperature loggers, Gama, 2015), or to access data from

98 specific locations and programs (i.e., TBEPtools for water quality data in the Tampa Bay, Beck  
99 et al., 2021; dataRetrieval for USGS gage and water quality data, DeCicco et al., 2024). Some  
100 packages exist to perform specific functions to sensor data regardless of data type (i.e., driftR to  
101 address drift in any sensor data, Shaughnessy et al., 2018; sensorQC to perform general QAQC  
102 checks and flagging, Read et al., 2015) or for the most commonly used sensor types (i.e.,  
103 sensorstrings for HOBO, Aquameasure, and Vemco buoy sensors, Dempsey, 2024;  
104 microclimloggers for iButton and HOBO pendant sensors, Boersch-Supan and Petry, 2018).  
105 However, these packages are not equipped to handle the altered data structure of raw data from  
106 STIC sensors. Additionally, few packages exist that contain both functions for processing and  
107 tidying data as well as QAQC functions that are sensor-specific. Therefore, STICr provides a  
108 FAIR framework for the entire process of data analysis for these increasingly common sensors.

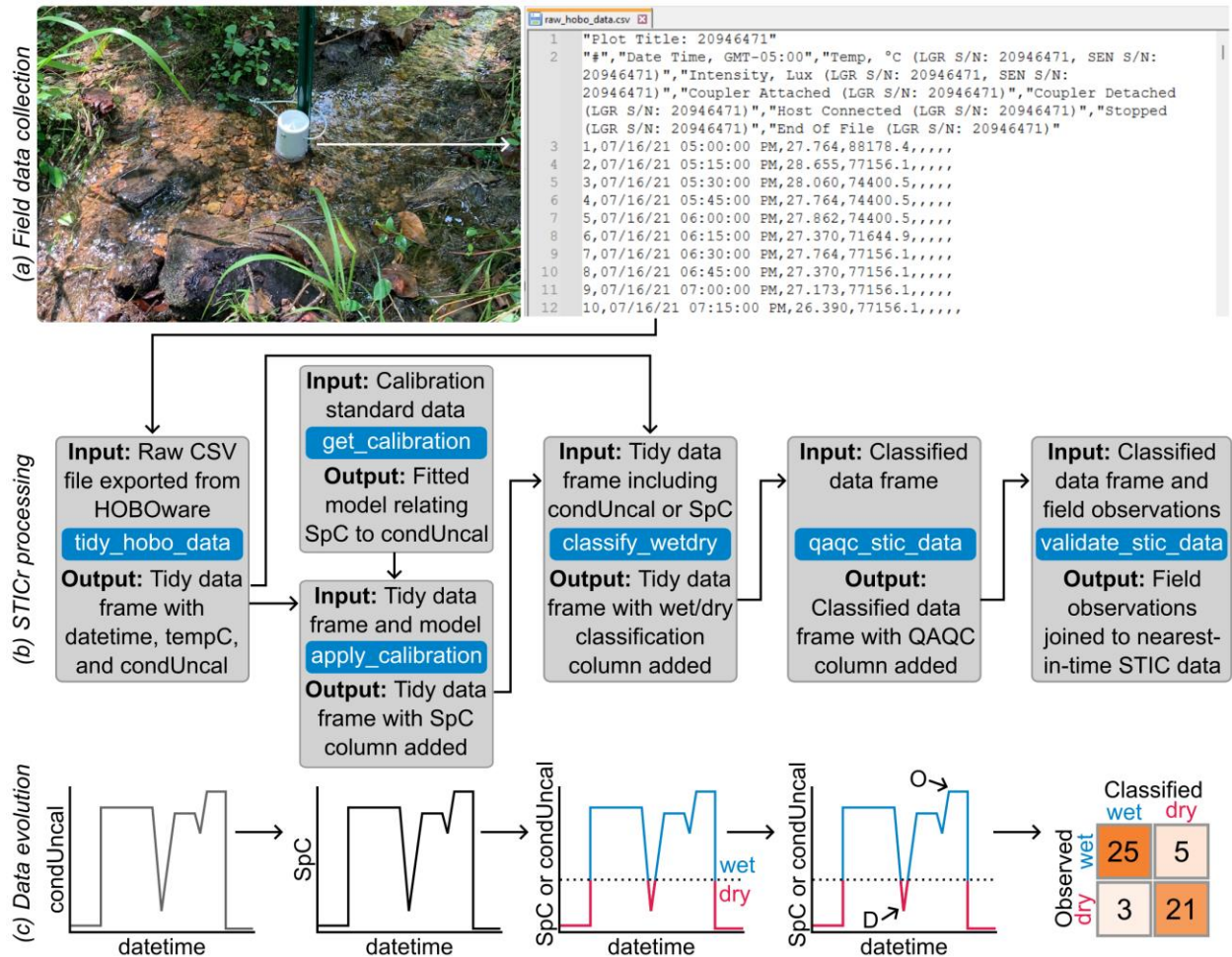
109 After describing STICr, we demonstrate how the package can be used in a project-  
110 specific reproducible workflow that involves processing data from many loggers spread across  
111 multiple watersheds and research groups to highlight a potential application of the STICr  
112 package. We then demonstrate how this can be used to understand links between hydroclimatic  
113 processes, geological processes, and spatiotemporal patterns of stream intermittency at the  
114 watershed scale, using the South Fork of Kings Creek at Konza Prairie Biological Station as an  
115 example.

116

## 117 **2. Methods: STICr functionality**

118 The overarching goal of the STICr package is to provide a workflow spanning five data  
119 processing steps (Figure 2): (1) “tidying” the raw HOBO output files such that basic data  
120 wrangling operations (i.e., subsetting, joining, etc.) can be performed easily; (2) converting the  
121 raw conductivity measured by the sensors into calibrated specific conductivity (SpC; units  
122  $\mu\text{S}/\text{cm}$ ); (3) interpreting the conductivity data into a binary “wet/dry” classification, indicating  
123 the presence or absence of water at the sensor at each timestep; (4) providing QAQC operations  
124 such as correcting negative calibrated conductivity values and flagging anomalous classification  
125 points; and (5) validating the classified STIC data and/or calibrated SpC data against field  
126 observations. STICr also includes sample datasets showing how these data look at each step in  
127 the workflow. After these operations are performed, the resulting data should be application-  
128 ready for hydrological analysis and can be more easily integrated with other datasets for analysis.  
129 In this section, we briefly describe the functionality of core STICr functions including input and  
130 output. In Section 3, we then show a project-specific application of this workflow.

131



132  
133 **Figure 1. STICr functionality from data collection to validation.** (a) Raw data collection, including a  
134 STIC logger deployed at a field site [photo credit: D.M. Peterson] and the resulting data output format  
135 from the proprietary HOBOWare software. (b) Core STICr functions shown in blue boxes, including  
136 input/output data and potential interlinkages among functions to create a processing workflow. (c) Visual  
137 depiction of how STIC data evolves as it moves through the STICr processing workflow. Variable names  
138 used in the figure include datetime = date and time of STIC reading, tempC = temperature in degrees  
139 Celsius, condUncal = uncalibrated relative conductivity logged by STIC, and SpC = specific conductivity.

140 **2.1 Step 1: Tidying output**

141 When the data from a logger is initially downloaded using the Onset HOBOWare  
142 proprietary interface and exported as a comma-separated value (CSV) file, it has many  
143 characteristics that make it inconvenient for analysis, including logger-specific column names  
144 with multiple spaces and punctuation marks, as well as metadata columns that do not represent  
145 actual observations (Figure 2a; example raw file available at  
146 [https://samzipper.com/data/raw\\_hobo\\_data.csv](https://samzipper.com/data/raw_hobo_data.csv)). The `tidy_hobo_data` function takes a raw CSV  
147 file exported from HOBOWare as input and produces a tidy data frame in the R global  
148 environment and/or a CSV file, as described below. The input data frame contains three key data  
149 columns (date and time of the observation, the uncalibrated conductivity measured by the sensor,

150 and the temperature in degrees Celsius measured by the sensor), which *tidy\_hobo\_data* preserves  
151 in the resulting output data frame. The output data frame has the following columns: *datetime*,  
152 which is the date and time of each observation; *condUncal*, which is the uncalibrated relative  
153 conductivity recorded by the STIC (unitless, though reported by Hoboware as “Lux” from the  
154 light sensor that is modified to record conductivity); and *tempC*, which is the temperature  
155 recorded by the STIC (units: Celsius).

## 156 2.2 Step 2 (optional): Calculation of Specific Conductivity (*SpC*)

157 Since STIC sensors are created from a modified light sensor, their conductivity data  
158 output is uncalibrated conductivity (*condUncal*), which is not a physically meaningful unit. Since  
159 STIC sensors can be used to monitor wet/dry conditions using their raw uncalibrated  
160 conductivity (Jensen et al., 2019), the calibration step is optional, but STIC calibration can  
161 provide more physically meaningful units (specific conductivity, or *SpC*) that are directly  
162 comparable between sensors and opens new research possibilities for investigating water quality  
163 dynamics, for example through high spatiotemporal resolution mapping of solute concentrations  
164 (Paillex et al., 2020).

165 In STICr, this is accomplished through two functions: *get\_calibration*, which develops a  
166 calibration curve from laboratory calibration data, and *apply\_calibration*, which applies the  
167 calibration curve to the tidied raw data to convert the *condUncal* recorded by the logger into  
168 physically meaningful *SpC*. In STICr, the *get\_calibration* function takes a data frame containing  
169 calibration data for a specific logger and outputs a fitted model object in R which relates lab-  
170 measured *SpC* to STIC-measured *condUncal*. Currently, *get\_calibration* creates a linear  
171 regression model, though other functional forms could be incorporated into the package in the  
172 future. This model object can be inspected to evaluate fit statistics ( $R^2$ , slope, intercept, etc.),  
173 uncertainty, and other properties useful to assess the performance of the calibration. The input  
174 STIC calibration data must be a data frame object with the following attribute labels: *standard*,  
175 referring to the *SpC* value (in  $\mu\text{S}/\text{cm}$ ) of a known standard in which the logger was submerged  
176 for calibration, and *condUncal*, referring to the corresponding measured conductivity logged by  
177 the STIC when submerged in the solution. Typically separate calibrations are required for each  
178 STIC sensor; a standard operating procedure (SOP) for STIC sensor calibration is provided in  
179 Burke et al. (2024).

180 The fitted model produced by *get\_calibration* can then be passed as an input argument to  
181 the *apply\_calibration* function, along with the tidied data generated in Step 1, to convert the  
182 STIC time series of *condUncal* to *SpC* using the *predict.lm* function from the ‘stats’ package for  
183 R. The function returns the same tidied data frame as the input, with the addition of an *SpC*  
184 column.

## 185 2.3 Step 3: Classifying wet/dry conditions

186 The *classify\_wetdry* function underlies the main purpose of STIC loggers, which is  
187 creating a binary “wet or dry” time series indicating the presence or absence of water at each

188 measurement timestep. The principle behind generating this data set is that conductivity (either  
189 *condUncal* or *SpC*) will be at or near zero when the electrodes of the sensor are in contact with  
190 air and will be at a high value if the electrodes are in contact with water. Despite the simplicity of  
191 this concept, there are several confounding factors that complicate this binary classification.  
192 These factors include the range of stream water conductivity conditions or the possibility that  
193 loggers may become buried in moist soil, both of which may lead to difficulty in interpreting  
194 where the cutoff is.

195 STICr's *classify\_wetdry* function takes a tidied STIC data frame as input, such as one  
196 generated by *tidy\_hobo\_data* or *apply\_calibration*. The user can then decide what column they  
197 would like to use for classification using the *classify\_var* input. While our project-specific  
198 workflow (detailed in Section 3) uses *condUncal* for wet/dry classification – since we did not  
199 have calibration data available for all STIC sensors – the *SpC* column can also be used. To  
200 account for the confounding factors described above, there are three choices of *method* for  
201 classification: (1) “*absolute*”, where the user must specify an absolute threshold of the  
202 classification variable; (2) “*percent*”, where the user specifies a percentage of the observed  
203 maximum value of the classification variable as a threshold (Warix et al., 2021), which can help  
204 account for sensor-specific differences in *condUncal* readings; or (3) “*y-intercept*”, in which the  
205 y-intercept of the fitted model developed in *get\_calibration* is used as a first-order approximation  
206 of the threshold (Bilbrey, 2024; Kindred, 2022). For each of these methods, values of the  
207 classification variable above the threshold are interpreted as wet and below the threshold are  
208 interpreted as dry.

209 The choice of the classification variable, method, and thresholds are important decisions  
210 and may vary widely in different environments, as typical *SpC* values in streams can span orders  
211 of magnitude across freshwater systems due to physiographic and environmental factors (Bolotin  
212 et al., 2023). In describing our project-specific case study, we show how a sensitivity analysis  
213 and validation process can be used to determine an appropriate classification threshold and  
214 evaluate the potential frequency and direction of misclassification errors (Section 3.4).  
215 Alternately, separate thresholds for each sensor could be developed and implemented using the  
216 STICr functionality. Ultimately, *classify\_wetdry* returns the same input data frame provided to  
217 the function with the addition of a new column called *wetdry*, which contains the character string  
218 “wet” or “dry” for every timestep.

#### 219 2.4 Step 4: Quality assurance/quality control (QAQC)

220 Once the STIC data are classified, the *qaqc\_stic\_data* function provides several options  
221 for typical QAQC procedures for stream intermittency data. The *qaqc\_stic\_data* takes in a  
222 classified data frame, as produced by the *classify\_wetdry* function, and allows the user to select  
223 different QAQC options that they may want to evaluate. Currently, there are three QAQC  
224 inspections available:

225 (1) Negative *SpC* values, which indicates an issue with the application of the calibration data to  
226 the field measurements. Most often the uncalibrated value associated with a negative *SpC*



227 is 0, indicating a high-confidence dry reading. As such, the *qaqc\_stic\_data* function gives  
228 users the option to set any negative *SpC* value to 0 and, if so, flag the data with the  
229 character “C”, for “Corrected”.

230 (2) Conductivity value outside the range of calibration standards (e.g. the calibrated *SpC* was  
231 estimated at 1200  $\mu\text{S}/\text{cm}$  but the highest concentration standard used during calibration was  
232 1000  $\mu\text{S}/\text{cm}$ ). This QAQC flag is produced in the *apply\_calibration* step when the fitted  
233 model is applied to the time series of STIC data. In this case, the data are flagged with the  
234 character code “O”, for “Outside”, but the value of *SpC* is not changed. As shown in  
235 Section 3.3, these data can be highly suspect when compared to field observations, so this  
236 flag is critical for potential interpretations of STIC *SpC* data.

237 (3) Short-term deviation in STIC classification data (e.g., a single “wet” data point surrounded  
238 by many “dry” data points before and after), likely indicating a potential sensor or  
239 classification anomaly. The anomaly detection takes as input two parameters: *window\_size*  
240 is a numeric argument specifying the number of observations that the anomaly must be  
241 surrounded by in order to be flagged, and *deviation\_size* specifies the maximum of a  
242 clustered group of points that will be flagged as an anomaly. Such anomalies are assigned  
243 the character code “D”, for “Deviation”. Since non-perennial streams can exhibit diel  
244 cycling between wet and dry conditions (Hale et al., 2024; Newcomb and Godsey, 2023;  
245 Warix et al., 2023), defining the appropriate *window\_size* and *anomaly\_size* require  
246 knowledge of the site’s expected stream drying and wetting regimes and typical local  
247 stream intermittency dynamics (Price et al., 2024, 2021).

248 The *qaqc\_stic\_data* function returns the same input data frame provided to the function with the  
249 addition of a new column called *QAQC*, which contains the flagging character codes (“C”, “O”,  
250 and “D”) that the user specified.

## 251 2.5 Step 5: Validation

252 The *validate\_stic\_data* function takes a data frame with field observations of wet/dry  
253 status and (optionally) measured *SpC* and aggregates STIC sensor data for these variables for  
254 STIC validation. The general purpose of the function is to test the accuracy of both the *SpC*  
255 conversion and classification. The input data frame of field observations must include a *datetime*  
256 column, as well as a column labeled *wetdry* consisting of the character strings “wet” or “dry” (as  
257 in the processed STIC data itself). Additionally, if independent field data on *SpC* were collected  
258 (e.g., with a sonde), this should be included as a third column in the observation data frame  
259 called *SpC*, and units should be in  $\mu\text{S}/\text{cm}$ . The *validate\_stic\_data* function then identifies the  
260 closest-in-time STIC sensor data (within a user-specific maximum allowed time range) and joins  
261 the relevant *wetdry*, *SpC*, and *QAQC* data collected by the STIC. Ultimately, this produces a new  
262 dataframe with columns for both the field observations (*wetdry\_obs*, *SpC\_obs*) and the  
263 corresponding STIC reading (*condUncal\_STIC*, *wetdry\_STIC*, *SpC\_STIC*, *QAQC\_STIC*). These  
264 data can then be used for a variety of different validation steps, such as accuracy assessments,



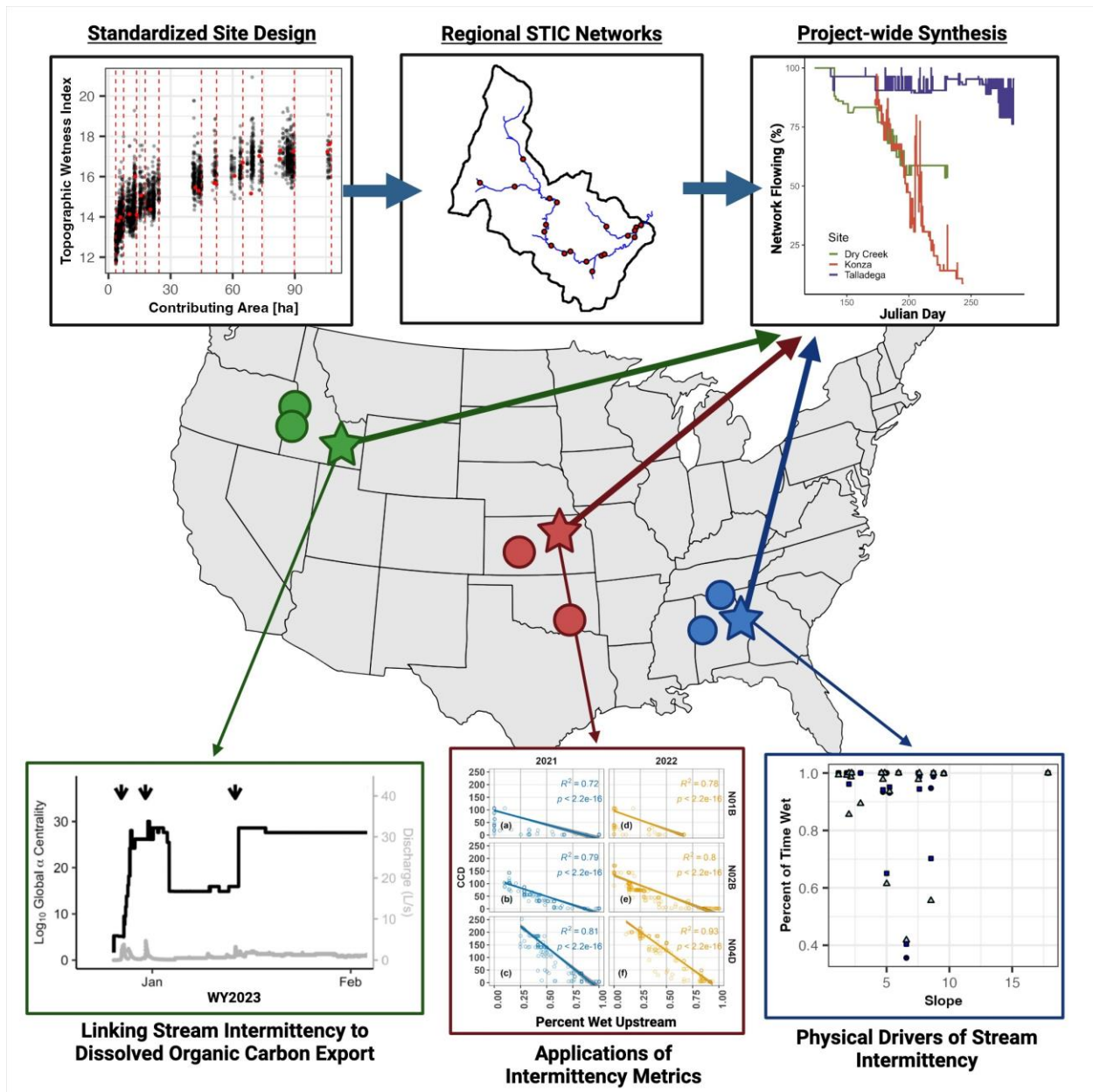
265 sensitivity analyses, and checking of calibration performance. Examples of each of these  
266 validation applications from the AIMS project are shown in Section 3.

### 267 **3. Case study: Integration into project-wide reproducible workflow**

#### 268 *3.1 Stream intermittency in a cross-institution interdisciplinary project*

269 Although the functions provided in STICr provide details tidying and processing operations,  
270 their arguments and functionality remain relatively general to allow users to adapt and integrate  
271 them into reproducible workflows that fit their specific needs. Here, we provide an example of  
272 how these functions are used in a reproducible workflow for organizing and processing STIC  
273 data for the *Aquatic Intermittency effects on Microbiomes in Streams* (AIMS) project, which  
274 includes over 200 STIC loggers from nine watersheds and multiple universities, investigators,  
275 and students over a multi-year period (Figure 2; Peterson et al., 2023). AIMS is a  
276 multidisciplinary National Science Foundation-funded project (award OIA-2019603) whose goal  
277 is to collect and integrate high resolution datasets on the hydrology, biogeochemistry, and  
278 microbial ecology of intermittent streams in multiple regions of the US. As such,  
279 methodologically consistent stream intermittency data from STIC loggers form the scientific  
280 backbone of this project to interpret variations in stream dissolved organic carbon export  
281 (Bilbrey, 2024), microbiome dynamics, macroinvertebrate community structure, and many other  
282 datasets being collected. This need for consistency in processing, analysis, and QAQC of STIC  
283 data across sites and regions, as well as the need to integrate this data with other project-specific  
284 data sets (e.g., optical water quality sensors, pressure transducers, etc.), led to the development of  
285 STICr and an AIMS-specific STIC data pipeline.

286  
287



288  
 289 **Figure 2. Design and application of STIC data for the AIMS project.** Each of the circles/stars on the  
 290 map is a study watershed where AIMS has deployed STIC sensors to monitor stream intermittency. The  
 291 sequence of plots along the top shows how a standardized site design, using topographic wetness index  
 292 and contributing area, was used to distribute the sensors within each watershed, and this consistent  
 293 approach allows for cross-site synthesis research. The graphs along the bottom show examples of region-  
 294 specific analyses that connect STIC data to other datasets being collected in the project. Top row figure  
 295 sources, from left to right: Peterson; Peterson; Kraft et al. (in prep). Bottom row figure sources, from left  
 296 to right: Bilbrey (2024), Ramos et al. (in prep), Peterson et al. (in prep).

297  
 298 **3.2 STIC data collection best practices**

299 The first step is the collection of high-quality field data. While the focus of this paper is  
 300 data analysis, we briefly offer several recommended best practices for field deployment to ensure

301 high data quality, and we have published SOPs on STIC deployment, maintenance, and  
302 calibration (Burke et al., 2024; Godsey et al., 2024). Prior to deployment, we recommend  
303 carefully calibrating the loggers using multiple solutions of known SpC that exceed the range of  
304 expected conditions in the field. As shown below (Section 3.4), STIC SpC estimates outside of  
305 the calibration range tend to perform quite poorly. We recommend a minimum of four  
306 calibration points encompassing the full range of SpC values that the STIC will likely encounter  
307 during its field deployment, including a dry calibration point when the STIC is exposed to the air  
308 rather than submerged in water. STICs can be re-calibrated as frequently as needed, for example  
309 during periods when they are being collected for download and redeployment. During  
310 deployment, the sensors should be placed in the stream thalweg with the sensor's electrodes just  
311 off the streambed to capture shallow flow (shown in Figure 1a). We typically place the sensor  
312 within two millimeters of the streambed, unless rapid sedimentation is expected, in which case  
313 positioning further above the streambed helps prevent sensor burial. Along the thalweg, specific  
314 sensor locations should be targeted based on the desired hydrologic indicators for the study, for  
315 example avoiding pools if the goal is to record the expansion and contraction of the surface water  
316 network in the catchment (Jensen et al., 2019) or targeting pools if the goal is to characterize the  
317 persistence of water in the network. The STICs should be visited regularly to check for erosion  
318 or sediment deposition, and to record a field observation of the wet/dry status and SpC which can  
319 be used for validation (Godsey et al., 2024). Finally, data from the sensors should be downloaded  
320 and sensors should be maintained on a regular schedule. We recommend downloading data and  
321 changing sensor batteries every 6 to 9 months. To assist with evaluation of the STIC data by  
322 other team members and researchers outside the project, we developed qualitative data quality  
323 categories, which are detailed in Appendix 1.

324

### 325 *3.3 Using STICr to create a FAIR data workflow*

326 The AIMS STIC processing workflow (Figure 3; available on GitHub,  
327 [https://github.com/HEAL-KGS/AIMS\\_stic\\_pipeline](https://github.com/HEAL-KGS/AIMS_stic_pipeline)) consists of five scripts written in R that  
328 make use of the *STICr* package by integrating the generalized functionality of *STICr* with  
329 additional project-specific requirements such as data naming and formatting conventions. While  
330 our analysis focuses on the widely used STIC sensor, apart from the *tidy\_hobo\_data* function,  
331 each of the functions and scripts we develop can also be modified to work with data from other  
332 stream intermittency sensors such as the Smart Rock (Milford and Truong, 2024).

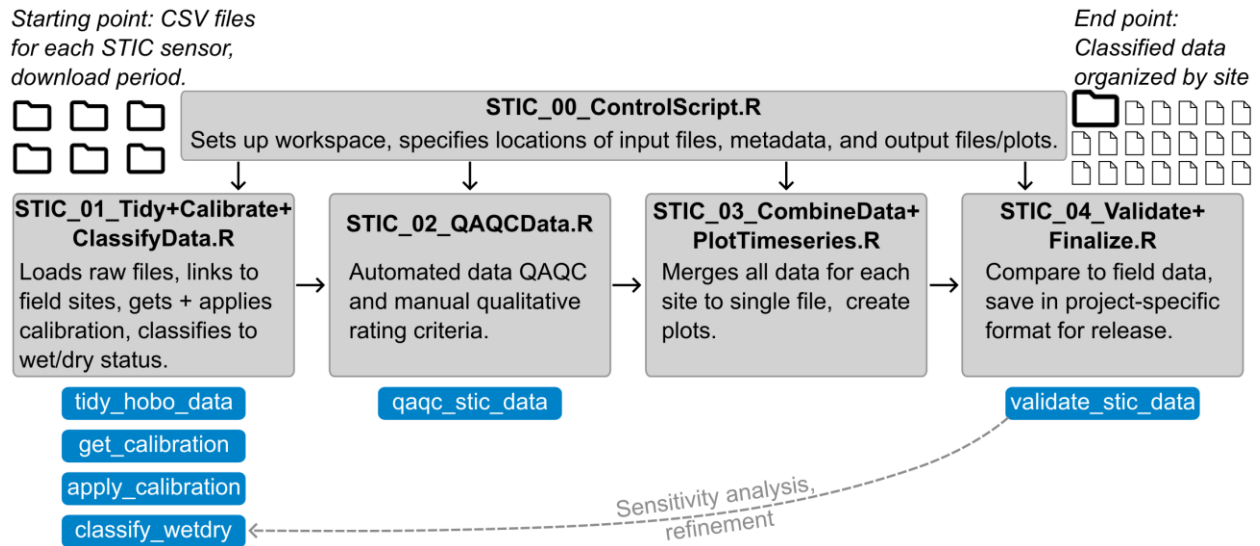
333 The AIMS pipeline is set up within the *STIC\_00\_ControlScript.R* script. In this script, the  
334 user defines the location of key files such as exported HOBO CSV data, a look-up table that  
335 links STIC serial numbers to specific field monitoring sites, calibration standard information, and  
336 paths to save output files and figures. Information from this control script is then read into each  
337 of the following four scripts that carry out sequential processing steps:

- 338 • *STIC\_01\_Tidy+Calibrate+ClassifyData.R* carries out the bulk of the processing,  
339 including the loading/tidying of raw HOBO CSV data (Step 1; Section 2.1), getting and  
340 applying the calibration to calculate *SpC* if available (Step 2; Section 2.2), and classifying

341 the STIC data to create the *wetdry* column (Step 3; Section 2.3). Due to the large number  
342 of loggers in use on this project and their different maintenance and download timelines,  
343 we perform the tidying, calibration, and classification on an entire folder of files that  
344 represents one set of STIC downloads at a particular site, which produces one CSV file  
345 per site, per download. We use a look-up table CSV file relating the serial number of the  
346 STIC logger to its project-specific site name (corresponding to its watershed position)  
347 This script also uses data contained within the CSVs to automate naming the output files  
348 according to the project-specific convention, which contains the logger serial number,  
349 site/region codes, and the start and end date/time for the download period in  
350 YYYYMMDD HH:MM:SS format.

- 351 • *STIC\_02\_QAQCdata.R* conducts both automated and manual QAQC steps. Automated  
352 steps include the corrections for negative estimated SpC values (“C” flag), identification  
353 of SpC values outside the range of standards used for calibration (“O” flag), and  
354 detection of deviations/anomalies in the classified time series (“D” flag). There is also a  
355 manual step in which the qualitative rating criteria are determined based on the  
356 conditions described in Appendix 1, which is streamlined through the importing of  
357 digitized STIC metadata sheets from field data collection efforts and the automated  
358 creation of diagnostic graphs and tables with information from the STIC sensor (i.e.,  
359 classified *wetdry* conditions, SpC, and *condUncal*) and corresponding field observations  
360 from the corresponding period. Plots produced by this script include time series of  
361 classified STIC *condUncal*, *tempC*, and *SpC* data, color-coded by wet/dry classification,  
362 which can be used for additional checks on classification performance. For example, the  
363 STIC daily temperature range is typically greater when the STIC is dry and exposed to  
364 the atmosphere than when it is when the STIC is wet and thermal variability is dampened  
365 by the water. Therefore, paired inspection of the temperature, conductivity, and  
366 classification data can be used to assess potential misclassification issues.
- 367 • *STIC\_03\_CombineData+PlotTimeseries.R* collects the classified and QAQCed data for  
368 each site across all download periods to produce a single CSV file, and associated  
369 summary plots, of all available data for each site. This script does not use any STICr  
370 functionality, but is necessary because different STIC loggers are used at the same site  
371 during different deployments.
- 372 • *STIC\_04\_Validate+Finalize.R* script compiles field observations and uses  
373 *validate\_stic\_data* to create the validation data frame, which is then plotted in various  
374 ways including a confusion matrix, sensitivity to threshold choice for *wetdry*  
375 classification, and overall accuracy. This script also creates additional data columns and  
376 saves the data into individual CSV files for each site and year to align with the AIMS  
377 project-wide data formatting standards. These are the files that are posted to HydroShare  
378 (Zipper et al., 2024).

379 Overall, the AIMS STIC data workflow shows one instance of how the generalized STICr  
380 functions can be utilized for the automation of project-specific tasks.



382

383

384

385

386

387

388

389

390

391

392

393

394

395

396

397

398

399

400

401

402

403

404

405

406

407

408

409

**Figure 3. STICr as part of a project-wide data processing workflow.** The starting point of the workflow is a set of raw CSV files exported from HOBOWare for each STIC download period. Each processing script is shown in a gray box with a summary of key steps, and STICr functions used in each script are shown beneath in blue. The end point is a classified and organized set of files for each site.

### 3.4 South Fork Kings Creek (Konza Prairie, Kansas, USA) STIC data

In this case study, we demonstrate an example of the implementation of STICr within the project-wide reproducible workflow to assess spatial and temporal patterns of stream intermittency in the South Fork Kings Creek watershed (Kansas, USA). This watershed is the core AIMS study watershed for the Great Plains region and is fully within the Konza Prairie Biological Station, which is host to a Long Term Ecological Research (LTER) site and is part of the National Ecological Observatory Network (NEON). Streamflow in the watershed is highly intermittent and characterized by a ‘fill-and-spill’ hydrology controlled by subsurface storage dynamics (Costigan et al., 2015). Subsurface hydrological processes are highly complex at the site due to the merokarst landscape typical of the Flint Hills ecoregion, which consists of thinly interbedded limestones (which act as aquifers through dissolution and fracture networks) and mudstones (which act as aquitards, but are highly fractured and likely leaky) (Macpherson, 1996; Vero et al., 2018). Overall, groundwater contributes a large portion of total streamflow (Hatley et al., 2023) but groundwater flowpaths are relatively rapid and grow longer as the stream network dries (Swenson et al., 2024). The spatial patterns of stream-aquifer interactions are complex, as water is exchanged between the stream and specific limestone units only in highly localized settings where limestones outcrop onto the streambed (Gambill et al., 2024) and the watershed groundwater system has complex potentiometric surfaces that are not exclusively driven by stream-aquifer interactions (Sullivan et al., 2020). While the ecoregion is native grassland, woody vegetation encroachment has expanded rapidly over the past several decades despite watershed burning and grazing, and has led to a decrease in annual streamflow despite increasing precipitation (Keen et al., 2024; Sadayappan et al., 2023).

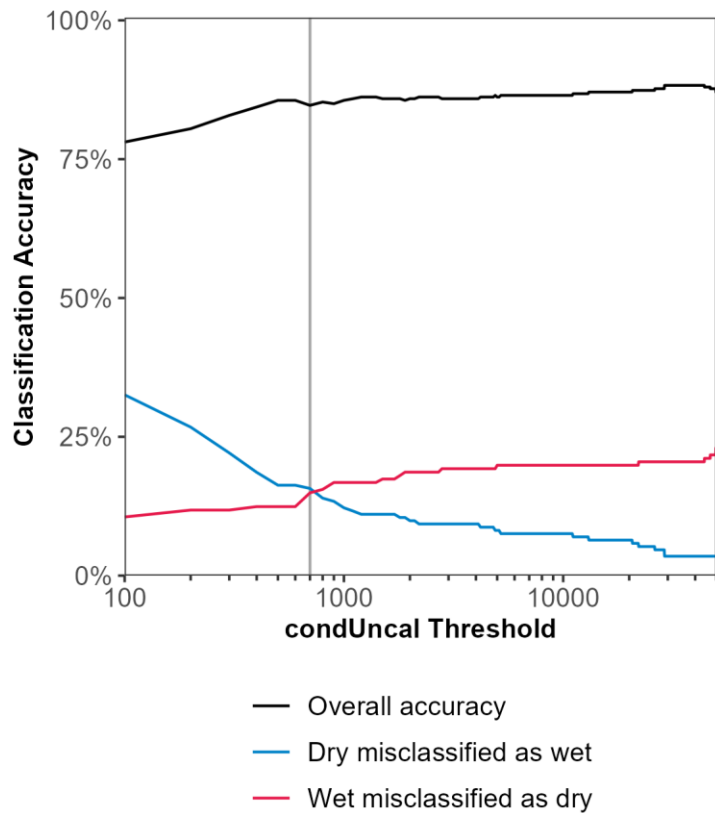
410 While this past work suggests potential spatial and temporal heterogeneity in streamflow  
411 dynamics, these studies have primarily focused on the outlets of four subwatersheds within South  
412 Fork Kings Creek that have streamflow gaging stations as part of the LTER program. In AIMS,  
413 we installed STIC sensors at 50 distributed locations within the South Fork Kings Creek  
414 watershed in May 2021, and data included in this study cover a three-year period from May 2021  
415 to May 2024. A detailed description of site selection is presented in Swenson et al. (2024).  
416 Briefly, some locations were identified based on local hydrologic site knowledge (such as the  
417 locations of springs and confluences) while others were randomly distributed to span a range of  
418 topographic wetness index (TWI) and drainage area (Figure 2), which past work has shown to be  
419 an important control over stream intermittency elsewhere (Warix et al., 2021). These locations  
420 were designed to balance project-wide goals related to hydrology, biogeochemistry,  
421 microbiology, and ecology, and therefore were not exclusively targeted towards stream  
422 intermittency efforts, but were driven by the overarching project goal of capturing a gradient of  
423 stream intermittency and hydrologic connectivity. At each site, the STIC was installed at the  
424 thalweg of a local channel high point, such as the top of a riffle sequence, so that a “wet” STIC  
425 reading would correspond to a connected stream network at that location (as opposed to the  
426 persistence of pools at the site). Most, but not all, STICs were calibrated before deployment and  
427 STICs were downloaded and maintained approximately every 6-9 months. During these visits,  
428 and at other opportunistic occasions when project members were collecting other field data at the  
429 sites, we collected field observations including wet/dry status and independent stream water SpC,  
430 for a total of 333 field observations that can be used for validation. The STIC field data  
431 collection followed the best practices described in Section 3.2 and data were processed using the  
432 workflow described in Section 3.3.

433

### 434 3.5 STIC data sensitivity analysis and validation

435 For the South Fork Kings Creek, we conducted an iterative sensitivity analysis and  
436 validation to determine the appropriate threshold for wet/dry classification. Since we did not  
437 have calibration data for all STIC sensors, we used *condUncal* for classification. To select the  
438 *condUncal* threshold used to identify wet and dry sensor readings in *classify\_wetdry*, we  
439 conducted a sensitivity analysis by evaluating agreement with observations using unitless  
440 *condUncal* thresholds every 100 from a low value of 100 to a high value of 100,000. At each  
441 threshold, we calculated overall classification accuracy (percent of field observations that agree  
442 with the closest-in-time STIC wet/dry classification), the percentage of dry field observations  
443 that were misclassified as wet, and the percentage of wet field observations that were  
444 misclassified as dry (Figure 4). We found that variability in the *condUncal* threshold had a  
445 relatively small influence on the overall classification accuracy, which is consistent with the  
446 strong conductivity contrast between air and water. However, there was an important trade-off  
447 with the type of misclassification errors, with lower *condUncal* threshold associated with a  
448 greater wet bias (dry observations misclassified as wet) and higher *condUncal* thresholds  
449 associated with a greater dry bias (wet observations misclassified as dry). For South Fork Kings

450 Creek, we selected a *condUncal* threshold of 700, which had a slightly lower overall  
 451 classification accuracy (84.7%) than the peak we found (max overall accuracy of 88.3% at a  
 452 *condUncal* threshold of 29,000), but minimized the difference between wet and dry  
 453 misclassification errors. This threshold was selected after consultation with other project  
 454 members who plan to use the STIC data in their analysis to best balance the potential types of  
 455 misclassification errors and avoid either dry or wet bias in the STIC data, demonstrating the  
 456 important role of project-wide communication in developing hydrological datasets for  
 457 interdisciplinary research goals. In practice, the best classification threshold will likely vary  
 458 between sensors, watersheds, and/or regions due to variability in sensor construction and  
 459 different conductivities of stream water. Therefore, overall classification accuracy could be  
 460 improved by developing sensor-specific wet/dry classification thresholds where resources  
 461 permit, which was completed for some AIMS watersheds. STICr provides a useful set of tools to  
 462 select this threshold, apply it to the STIC data, and evaluate its accuracy.  
 463



464  
 465 **Figure 4. Selecting optimal classification threshold for the South Fork Kings Creek (Konza Prairie)**  
 466 **watershed.** This figure shows the overall classification accuracy as well as the proportion of different  
 467 types of misclassification errors as a function of the *condUncal* threshold used in the *classify\_wetdry*  
 468 function. The gray vertical line (*condUncal* = 700) was used for watershed-wide classification.  
 469

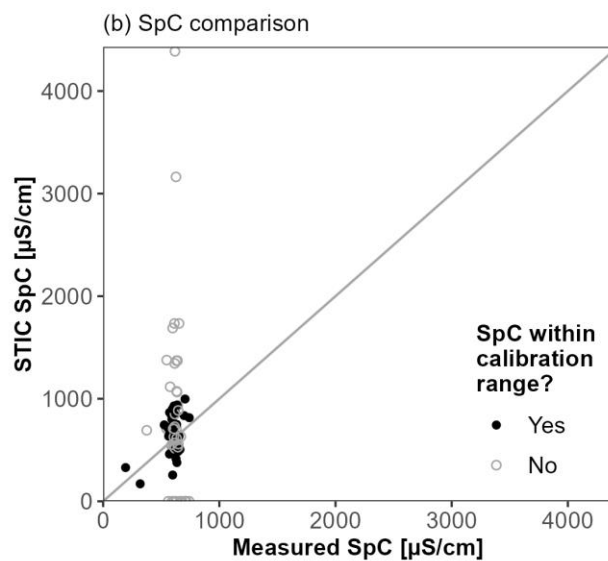
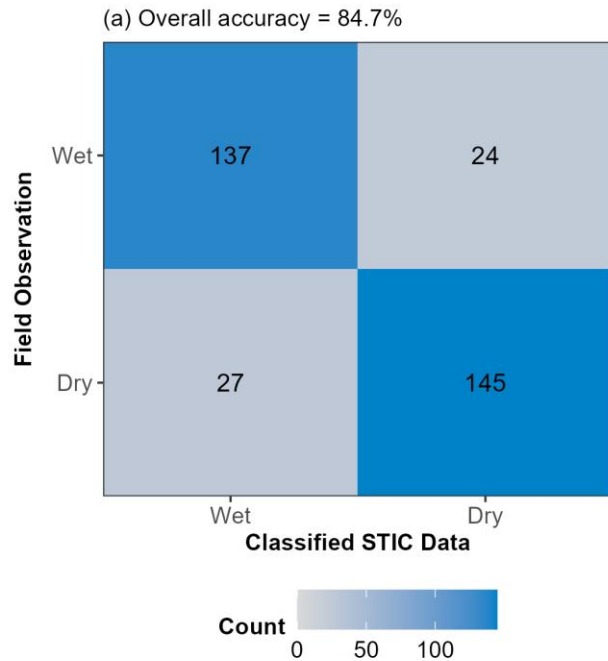
470 Overall, the total classification accuracy was 84.7% and had relatively balanced data  
 471 between correctly classified wet/dry conditions (137 and 145 correctly classified observations,



472 respectively) and incorrectly classified wet/dry errors (24 and 27 observation errors,  
473 respectively) (Figure 5a). Of the 24 wet observations that were misclassified as dry, 13 of them  
474 had a *condUncal* reading of 0, suggesting that the misclassification was caused by the STIC  
475 being out of the water, for example due to channel erosion or migration. For the remaining wet  
476 observations misclassified as dry, a lower classification threshold could have fixed the issue,  
477 suggesting potential value from sensor-specific accuracy assessments and classification threshold  
478 determination.

479         However, the agreement between field-measured SpC values and calibrated STIC  
480 observed SpC data was poor, with much higher SpC values estimated from the STICs than  
481 observed in the field-measured SpC. This comparison demonstrates the value of our QAQC  
482 procedures, as screening out any data points flagged with a “C” (meaning negative SpC values  
483 were obtained after calibration) or an “O” (meaning the calibrated SpC was outside the range of  
484 standards) eliminates the most extreme SpC values, which are shown as gray circles in Figure  
485 5b. The remaining data points are distributed close to the 1:1 line (slope = 0.998), though the  
486 overall coefficient of determination remains relatively low ( $R^2 = 0.20$ ) compared to lab fits to  
487 calibration standards, which generally had an  $R^2 > 0.9$ . The lower agreement compared to field  
488 could be due to issues with the STIC calibrations (such as calibration drift through time), issues  
489 with the STIC *condUncal* raw data (such as biofouling of the STIC electrodes during deployment  
490 which could influence conductivity), or issues with the field observations (such as errors in  
491 portable water quality sondes used to measure SpC). Through this validation process, we can  
492 constrain the potential applications of STIC-derived SpC data and identify potential  
493 opportunities to improve future calibration and data collection practices.

494

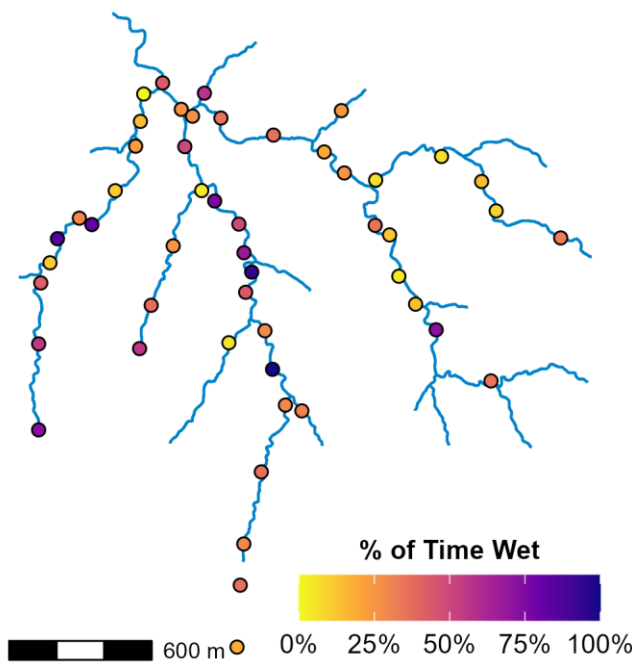


495  
 496 **Figure 5. STIC data validation from the South Fork Kings Creek (Konza Prairie) watershed.** (a)  
 497 Confusion matrix showing classification accuracy. The numbers correspond to the total number of  
 498 observations in each quadrant. (b) Scatterplot showing calibrated SpC accuracy.

499  
 500 *3.5 Spatial and temporal intermittency dynamics*

501 Our STIC data collection, which was motivated by the goal to develop improved  
 502 understanding of spatial patterns of stream intermittency at a watershed scale (Section 3.1),  
 503 revealed both spatial and temporal of stream intermittency dynamics in South Fork Kings Creek.  
 504 Spatially, we observed that the South Fork Kings Creek watershed generally has the wettest  
 505 conditions (greatest percent of time wet) in the middle reaches of the westernmost subwatersheds  
 506 in the study area, while conditions are drier in the upstream and downstream portions and

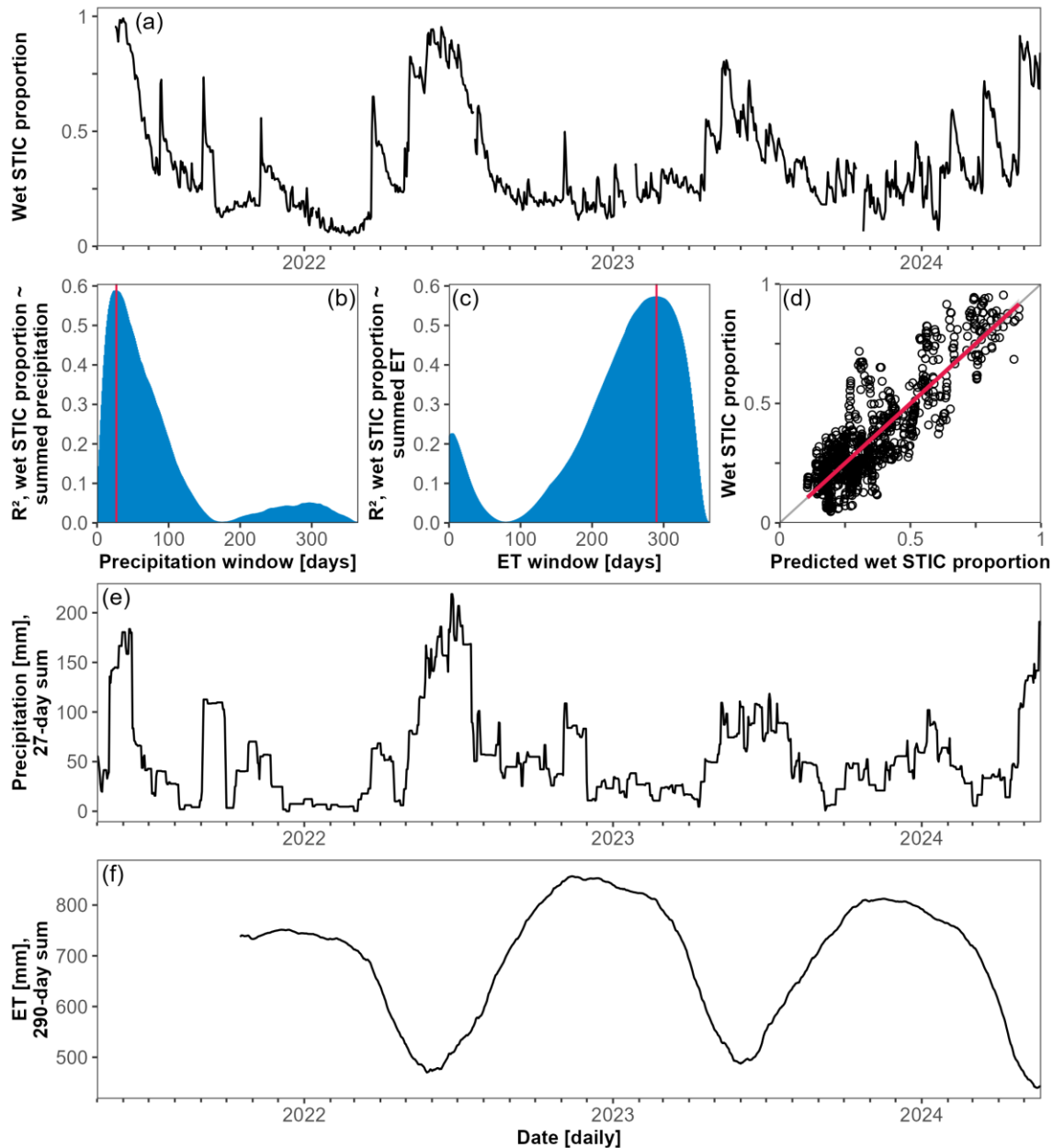
507 easternmost subwatersheds (Figure 6). The locations with the greatest flow persistence are  
508 associated with portions of the stream network where past work has found significant local  
509 contributions from limestone aquifers and the stream channel, while downstream areas with less  
510 flow persistence are associated with potential areas of loss from the aquifer into the stream  
511 (Gambill et al., 2024). Since flow at the watershed outlet tends to be dominated by groundwater  
512 (Hatley et al., 2023), but with relatively high fractions of young water (water that fell as  
513 precipitation within the past three months; Swenson et al., 2024), this supports the important role  
514 of fill-and-spill dynamics within specific limestone aquifers as key controls over flow persistence  
515 not just at the watershed outlet, as shown by Costigan et al. (2015), but also at fine spatial  
516 resolution within the stream network.  
517



518  
519 **Figure 6. Spatial patterns of stream intermittency.** Map of the South Fork of Kings Creek STIC  
520 monitoring network, colored by the percentage of time that each STIC was classified as wet conditions  
521 for the May 2021 to May 2024 period of record.

522  
523 From a temporal perspective, the classified STIC data reveals a highly dynamic  
524 watershed that is rarely completely wet and never completely dry (Figure 7a). Stream wetting  
525 tends to be flashy, with immediate increases in the wet STIC proportion associated with  
526 precipitation events, and then more gradual recessions back to a relatively consistent baseline of  
527 ~10-20% wet STICs, which are primarily concentrated in the middle portions of the watershed  
528 (Figure 6). To investigate climatic drivers of intermittency, we obtained daily meteorological  
529 data from the Konza Prairie LTER (Nippert, 2024) and daily watershed-average  
530 evapotranspiration (ET) data from OpenET, which provides satellite-derived estimates of daily  
531 ET for the western US (Melton et al., 2022; Volk et al., 2024), and tested the linear correlation

532 between each of these climatic drivers summed over time lags ranging from 1 to 365 days. This  
533 reveals that temporal patterns of network-scale stream intermittency are strongly associated with  
534 the atmospheric water supply (precipitation) and losses (ET) at different timescales. The best  
535 predictive relationships for wet STIC proportion occur when precipitation is summed over the  
536 prior 27 days ( $R^2 = 0.59$ ; Figure 7b, Figure 7e) and when ET is summed over the prior 290 days  
537 ( $R^2 = 0.57$ ; Figure 7c, Figure 7f). A simple multiple linear regression model using these two  
538 variables as predictors can explain 75% of the overall variability in wet STIC proportion (Figure  
539 7d), with a significant ( $p < 0.05$ ) positive relationship to 27-day summed precipitation and a  
540 significant negative relationship to 290-day summed ET.



542

543 **Figure 7. Temporal patterns and drivers of stream intermittency.** (a) Daily wet STIC proportion for544 the May 2021 – May 2024 period (tick marks show months).  $R^2$  of a linear relationship between the

545 proportion of wet STICs and (b) summed precipitation and (c) summer ET for different windows. (d)

546 Predicted wet STIC proportion as a function of precipitation over the preceding 27-day window (best for

547 from panel b;  $R^2 = 0.59$ ) and ET over the preceding 290-day window (best for panel c;  $R^2 = 0.57$ ), with548 gray line showing 1:1 relationship and red line showing linear best fit (overall  $R^2 = 0.75$ ). Daily time

549 series of (e) summed 27-day precipitation and (f) summer 290-day ET.

550

## 551 4. Discussion

### 552 4.1 STICr functionality and future development needs

553 Although the package presented here represents an important first step toward an open  
554 and reproducible framework for stream intermittency sensors, it is an ongoing package with  
555 several opportunities for improvement. First, while the *classify\_wetdry* function allows for  
556 several different approaches to differentiate wet and dry sensor data, it does not currently take  
557 advantage of temperature data, which is an additional dataset recorded by STIC sensors that can  
558 be used for identifying dry and wet periods (Constantz et al., 2001). Second, STIC data can often  
559 have gaps due to sensor malfunction or loss, which can lead to difficulties in calculated derived  
560 metrics that depend on complete data such as communication distance (Aho et al., 2023),  
561 longitudinal connectivity (Zimmer and McGlynn, 2018), or active drainage density (Godsey and  
562 Kirchner, 2014). Work elsewhere has suggested that stream network length is often hierarchical,  
563 meaning that sites dry and rewet in a typical order (Botter et al., 2021; Botter and Durigetto,  
564 2020), and integrating this concept into STICr as a potential gap-filling approach (with  
565 appropriate flags in the QAQC column) would improve STICr's ability to develop spatially and  
566 temporally complete datasets of stream intermittency (Durigetto et al., 2023). Third, the  
567 package currently relies on manual reading and export of data from the proprietary HOBOWare  
568 format to a machine-readable CSV format, and development of a programming-based approach  
569 to read in the HOBOWare files directly would enhance reproducibility and efficiency. As an  
570 open-source package, we encourage STIC users to address these needs and/or make additional  
571 suggestions for improvements as issues on the package GitHub page ([https://github.com/HEAL-](https://github.com/HEAL-KGS/STICr/issues)  
572 [KGS/STICr/issues](https://github.com/HEAL-KGS/STICr/issues)) and contribute code they develop for their own analyses.

573

### 574 4.2 Integration into interdisciplinary research projects

575 Using STICr, we demonstrate how a workflow can be developed to create FAIR and  
576 standardized stream intermittency data (Figure 3) for a project spanning multiple watersheds,  
577 institutions, and personnel (Figure 2). Since each watershed had different personnel, sensor  
578 deployment and maintenance timelines, and ability to access sites, the modular approach enabled  
579 by STICr allowed for the development of consistent processing workflows with site-specific  
580 modifications where needed as the project evolved. Given the increasing interdisciplinary  
581 collaboration around non-perennial stream research, hydrological flow intermittence data is  
582 increasingly of interest to researchers in disciplines such as ecology (Allen et al., 2020; Datry et  
583 al., 2018; DelVecchia et al., 2022), and biogeochemistry (Price et al., 2024; Ward et al., 2019;  
584 Zimmer et al., 2022). Here, we demonstrate how STICr's functionality can be used to carry out  
585 sensitivity analyses and validations that quantify the impacts of different hydrologic data  
586 processing decisions on potential classification errors (Figure 4). These types of decisions are  
587 often hidden in derived data products, and we show how STICr provides a quantitative  
588 framework that researchers can use to gather feedback and make collaborative decisions about  
589 data processing steps that meet the needs of eventual data users from other disciplines.  
590 Additionally, the standardized approach to QAQC flagging allows future users of the data,

591 whether within or beyond the project, to make important data filtering decisions and  
592 interpretations based on their research questions and data needs (Figure 5).

593

#### 594 *4.3 Evaluating spatial and temporal stream intermittency dynamics*

595 We also present a brief case study demonstrating how data processed using STICr can be  
596 used to assess spatial and temporal dynamics of stream intermittency in the South Fork Kings  
597 Creek watershed (Kansas, USA). We documented complex spatial patterns in watershed-scale  
598 stream intermittency (Figure 6), with the greatest wetness in the middle portion of the watershed  
599 and drier conditions upstream and downstream. We interpret these spatial patterns to be driven  
600 by localized stream-aquifer exchange that are ultimately controlled by the intersection of  
601 different limestone units with the stream channel (Gambill et al., 2024; Macpherson, 1996; Vero  
602 et al., 2018). This finding supports work done in sedimentary river systems documenting fine-  
603 scale variation in stream-aquifer exchange driven by streambed properties (Noorduyn et al.,  
604 2014; Shanafield et al., 2020b), and suggests that flow at the watershed outlet may not always be  
605 a direct indicator of hydrologic function, and associated water quality outcomes. As a result,  
606 network-scale stream connectivity indicators such as active channel length (Botter et al., 2021)  
607 and communication distance (Aho et al., 2023), informed by data from stream intermittency  
608 sensors like STICs, will likely play a critical role in determining the drivers of water quantity and  
609 quality impacts of non-perennial streams – a major open question in hydrologic research  
610 (Shanafield et al., 2020a; Zimmer et al., 2022).

611 Our investigation of temporal dynamics showed a time-varying meteorological response  
612 to controlling hydroclimatic variables, with a shorter (27-day) correlation with precipitation and  
613 a longer (290-day) correlation with ET in the watershed. These two timescales combined to  
614 produce rapid, precipitation event-driven wetting superimposed on a seasonal wetting and drying  
615 pattern created by the cumulative water use of vegetation throughout the summer and fall. This  
616 sheds light on climatic controlling the wetting and drying regime at this site, which have strong  
617 potential impacts on biogeochemical and ecological function (Price et al., 2024, 2021), and can  
618 vary at fine spatial scales (Sabathier et al., 2023). Both climate and land cover are changing in  
619 the region, with a long-term increasing precipitation trend counteracted by increased ET due to  
620 woody vegetation encroachment (Sadayappan et al., 2023). There is increasing evidence that  
621 non-perennial stream ecosystems can be characterized by alternative ecohydrological stable  
622 states (Ayers et al., 2024; Dodds et al., 2023; Heffernan, 2008; Zipper et al., 2022) with  
623 nonlinear trajectories of change (Kar et al., 2024), suggesting that the interactions among  
624 concurrent changes in precipitation and ET could drive regime shifts to novel hydrologic regimes  
625 in the future.

626

## 627 **5. Conclusions**

628 In this study, we introduced STICr, an open-source R package for working with Stream  
629 Temperature, Intermittency, and Conductivity (STIC) data. STICr includes a variety of functions  
630 for tidying, calibrating, QAQCing, and validating STIC data in order to advance FAIR stream



631 intermittency data. We then provided a case study showing how STICr can be incorporated into a  
632 workflow for processing STIC data on a cross-regional interdisciplinary project, and how STICr  
633 capabilities related to validation and sensitivity analysis can be used to make data processing  
634 decisions that prioritize the needs to future data users. The stable version of STICr is currently  
635 available on the Comprehensive R Archive Network (CRAN; [https://cran.r-](https://cran.r-project.org/package=STICr)  
636 [project.org/package=STICr](https://cran.r-project.org/package=STICr)) and the development version is available on GitHub  
637 (<https://github.com/HEAL-KGS/STICr>) and we welcome contributions from the community.

638 For the South Fork Kings Creek watershed (Kansas, USA), we used the data produced by  
639 this workflow to show spatial and temporal dynamics of stream intermittency over a three-year  
640 study period. We found that the watershed stays wettest for the longest duration in the middle  
641 and western portions, which are areas where outcropping limestone aquifers intersect the aquifer.  
642 At the network-scale, we show that the proportion of the network that is wet at a daily timestep  
643 can be well-predicted by precipitation over an approximately monthly timescale (27 days) and  
644 ET over a longer period (290 days) that is associated with the cumulative water uptake by plants  
645 over the growing season. Combined, these timescales lead to rapid increases in hydrologic  
646 connectivity in response to precipitation events and gradual recessions in response to seasonal  
647 network drying. The functions here, and associated shared workflows, provide a valuable basis  
648 for developing FAIR stream intermittency datasets and advancing links between non-perennial  
649 stream hydrology and other disciplines.

650

## 651 **Software and data availability**

- 652 • STICr:
  - 653 ○ Release version (v1.1): <https://cran.r-project.org/package=STICr>
  - 654 ○ Development version: <https://github.com/HEAL-KGS/STICr>
- 655 • AIMS STIC processing workflow: [https://github.com/HEAL-KGS/AIMS\\_stic\\_pipeline](https://github.com/HEAL-KGS/AIMS_stic_pipeline)
- 656 • South Fork Kings Creek raw STIC data:
  - 657 <http://www.hydroshare.org/resource/77d68de62d6942ceab6859fc5541fd61> (Zipper et al.,  
658 2024)
- 659 • Code and data used to generate the figures in this manuscript:
  - 660 [https://github.com/samzipper/AIMS\\_STIC\\_GP](https://github.com/samzipper/AIMS_STIC_GP)
  - 661 ○ This will be placed into a repository with a DOI at the time of manuscript  
662 acceptance so a DOI-ed dataset will be included in the final manuscript

## 663 **CRedit authorship contribution statement**

664 SZ: Conceptualization, Data curation, Formal analysis, Funding acquisition, Investigation,  
665 Methodology, Project administration, Resources, Software, Supervision, Validation,  
666 Visualization, Writing-Original Draft, Writing-Review & Editing

667

668 CTW: Conceptualization, Data curation, Formal analysis, Investigation, Methodology, Software,  
669 Supervision, Validation, Visualization, Writing-Original Draft, Writing-Review & Editing

670  
671  
672  
673  
674  
675  
676  
677  
678  
  
679  
680  
681  
682  
  
683  
684  
685  
686  
687  
688  
  
689  
690  
691  
692  
693  
694  
695  
696  
697  
698  
699  
700  
701  
702  
703  
704  
705  
706  
707  
  
708

DMP: Methodology, Software, Visualization, Writing-Review & Editing

SCC: Data curation, Methodology, Software, Writing-Review & Editing

SEG: Funding acquisition, Methodology, Supervision, Writing-Review & Editing

KA: Funding acquisition, Methodology, Writing-Review & Editing

### **Declaration of competing interest**

The authors declare no competing financial interests or personal relationships that could appear to influence the work reported in this paper.

### **Acknowledgments**

This work was supported by National Science Foundation award OIA-2019603. We appreciate feedback on STICr code and use from Naomi Anderson, Anna Bergstrom, Connor Brown, Thane Kindred, Maggi Kraft, Alexi Sommerville, and the rest of the AIMS team. STICr and associated workflows make heavy use of the Tidyverse family of R packages (Wickham et al., 2019).

### **Appendix 1: STIC qualitative rating criteria**

The following definitions were adopted by the AIMS project to rate the quality of STIC data for a given download period:

- **Excellent:** STIC was (1) calibrated prior to deployment, and (2) stayed operational throughout 95% of the download period, and (3) was not displaced from streambed (i.e., the external electrodes were within 1 cm from stream bed at the time of download indicating minimal erosion/deposition), and (4) data from sensor roughly agree with field observations of wet/dry (i.e., >1000 Lux sensor reading on day of removal corresponds to field observations of water at STIC).
- **Good:** (1) STIC stayed operational throughout the entire download period, and (2) the external electrodes were within 1 cm from stream bed at the time of download, and (3) data from sensor roughly agree with field observations of wet/dry, but (4) the STIC was not calibrated prior to deployment.
- **Fair:** (1) STIC stayed operational throughout 75% or more of the download period, and (2) data roughly agree with field observations, and/or (3) the external electrodes were between 1-3 cm from streambed at the time of download.
- **Poor:** (1) STIC stayed operational throughout less than 75% of the download period, and/or (2) the external electrodes were >3 cm from streambed at the time of download, and/or (3) data does NOT agree with field observations.

709 **References**

- 710 Aho, K., Derryberry, D., Godsey, S.E., Ramos, R., Warix, S.R., Zipper, S., 2023.  
711 Communication Distance and Bayesian Inference in Non-Perennial Streams. *Water*  
712 *Resources Research* 59, e2023WR034513. <https://doi.org/10.1029/2023WR034513>
- 713 Aho, K.S., Maavara, T., Cawley, K.M., Raymond, P.A., 2023. Inland Waters can Act as Nitrous  
714 Oxide Sinks: Observation and Modeling Reveal that Nitrous Oxide Undersaturation May  
715 Partially Offset Emissions. *Geophysical Research Letters* 50, e2023GL104987.  
716 <https://doi.org/10.1029/2023GL104987>
- 717 Allen, D.C., Datry, T., Boersma, K.S., Bogan, M.T., Boulton, A.J., Bruno, D., Busch, M.H.,  
718 Costigan, K.H., Dodds, W.K., Fritz, K.M., Godsey, S.E., Jones, J.B., Kaletova, T.,  
719 Kampf, S.K., Mims, M.C., Neeson, T.M., Olden, J.D., Pastor, A.V., Poff, N.L., Ruddell,  
720 B.L., Ruhi, A., Singer, G., Vezza, P., Ward, A.S., Zimmer, M., 2020. River ecosystem  
721 conceptual models and non-perennial rivers: A critical review. *WIREs Water* 7, e1473.  
722 <https://doi.org/10.1002/wat2.1473>
- 723 Ayers, J.R., Yarnell, S.M., Baruch, E., Lusardi, R.A., Grantham, T.E., 2024. Perennial and Non-  
724 Perennial Streamflow Regime Shifts Across California, USA. *Water Resources Research*  
725 60, e2023WR035768. <https://doi.org/10.1029/2023WR035768>
- 726 Beck, M.W., Schrandt, M.N., Wessel, M.R., Sherwood, E.T., Raulerson, G.E., Prasad, A.A.B.,  
727 Best, B.D., 2021. tbeptools: An R package for synthesizing estuarine data for  
728 environmental research. *Journal of Open Source Software* 6, 3485.  
729 <https://doi.org/10.21105/joss.03485>
- 730 Bilbrey, E.M., 2024. Quantifying Dissolved Organic Carbon Patterns and the Impact of Stream  
731 Network Connectivity on Export From Semi-Arid Intermittent Watersheds (M.S.). Idaho  
732 State University, United States -- Idaho.
- 733 Boersch-Supan, P., Petry, W., 2018. microclimloggers.
- 734 Bolotin, L.A., Summers, B.M., Savoy, P., Blaszczyk, J.R., 2023. Classifying freshwater salinity  
735 regimes in central and western U.S. streams and rivers. *Limnology and Oceanography*  
736 *Letters* 8, 103–111. <https://doi.org/10.1002/lo2.10251>
- 737 Botter, G., Durighetto, N., 2020. The Stream Length Duration Curve: A Tool for Characterizing  
738 the Time Variability of the Flowing Stream Length. *Water Resources Research* 56,  
739 e2020WR027282. <https://doi.org/10.1029/2020WR027282>
- 740 Botter, G., Vingiani, F., Senatore, A., Jensen, C., Weiler, M., McGuire, K., Mendicino, G.,  
741 Durighetto, N., 2021. Hierarchical climate-driven dynamics of the active channel length  
742 in temporary streams. *Sci Rep* 11, 21503. <https://doi.org/10.1038/s41598-021-00922-2>
- 743 Brinkerhoff, C.B., Gleason, C.J., Kotchen, M.J., Kysar, D.A., Raymond, P.A., 2024. Ephemeral  
744 stream water contributions to United States drainage networks. *Science* 384, 1476–1482.  
745 <https://doi.org/10.1126/science.adg9430>
- 746 Burke, E., Wilhelm, J., Zipper, S., Brown, C., 2024. AIMS SOP STIC Calibration.
- 747 Busch, M.H., Boersma, K.S., Cook, S.C., Jones, C.N., Loflen, C., Mazor, R.D., Stancheva, R.,  
748 Price, A.N., Stubbington, R., Zimmer, M.A., Allen, D.C., 2024. Macroinvertebrate, algal  
749 and diatom assemblages respond differently to both drying and wetting transitions in non-  
750 perennial streams. *Freshwater Biology* 69, 1568–1582. <https://doi.org/10.1111/fwb.14327>
- 751 Chapin, T.P., Todd, A.S., Zeigler, M.P., 2014. Robust, low-cost data loggers for stream  
752 temperature, flow intermittency, and relative conductivity monitoring. *Water Resour.*  
753 *Res.* n/a-n/a. <https://doi.org/10.1002/2013WR015158>

754 Constantz, J., Stonestorm, D., Stewart, A.E., Niswonger, R., Smith, T.R., 2001. Analysis of  
755 streambed temperatures in ephemeral channels to determine streamflow frequency and  
756 duration. *Water Resources Research* 37, 317–328.  
757 <https://doi.org/10.1029/2000WR900271>

758 Costigan, K.H., Daniels, M.D., Dodds, W.K., 2015. Fundamental spatial and temporal  
759 disconnections in the hydrology of an intermittent prairie headwater network. *Journal of*  
760 *Hydrology* 522, 305–316. <https://doi.org/10.1016/j.jhydrol.2014.12.031>

761 Datry, T., Foulquier, A., Corti, R., von Schiller, D., Tockner, K., Mendoza-Lera, C., Clément,  
762 J.C., Gessner, M.O., Moleón, M., Stubbington, R., Gücker, B., Albariño, R., Allen, D.C.,  
763 Altermatt, F., Arce, M.I., Arnon, S., Banas, D., Banegas-Medina, A., Beller, E.,  
764 Blanchette, M.L., Blanco-Libreros, J.F., Blessing, J.J., Boëchat, I.G., Boersma, K.S.,  
765 Bogan, M.T., Bonada, N., Bond, N.R., Brintrup Barría, K.C., Bruder, A., Burrows, R.M.,  
766 Cancellario, T., Canhoto, C., Carlson, S.M., Cauvy-Fraunié, S., Cid, N., Danger, M., de  
767 Freitas Terra, B., De Girolamo, A.M., de La Barra, E., del Campo, R., Diaz-Villanueva,  
768 V.D., Dyer, F., Elosegí, A., Faye, E., Febria, C., Four, B., Gafny, S., Ghate, S.D., Gómez,  
769 R., Gómez-Gener, L., Graça, M.A.S., Guareschi, S., Hoppeler, F., Hwan, J.L., Jones, J.I.,  
770 Kubheka, S., Laini, A., Langhans, S.D., Leigh, C., Little, C.J., Lorenz, S., Marshall, J.C.,  
771 Martín, E., McIntosh, A.R., Meyer, E.I., Miliša, M., Mlambo, M.C., Morais, M., Moya,  
772 N., Negus, P.M., Niyogi, D.K., Papatheodoulou, A., Pardo, I., Pařil, P., Pauls, S.U.,  
773 Pešić, V., Poláček, M., Robinson, C.T., Rodríguez-Lozano, P., Rolls, R.J., Sánchez-  
774 Montoya, M.M., Savić, A., Shumilova, O., Sridhar, K.R., Steward, A.L., Storey, R.,  
775 Taleb, A., Uzan, A., Vander Vorste, R., Waltham, N.J., Woelfle-Erskine, C., Zak, D.,  
776 Zarfl, C., Zoppini, A., 2018. A global analysis of terrestrial plant litter dynamics in non-  
777 perennial waterways. *Nature Geosci* 11, 497–503. [https://doi.org/10.1038/s41561-018-](https://doi.org/10.1038/s41561-018-0134-4)  
778 [0134-4](https://doi.org/10.1038/s41561-018-0134-4)

779 DeCicco, L., Hirsch, R., Lorenz, D., Read, J., Walker, J., Platt, L., Watkins, D., Blodgett, D.,  
780 Johnson, M., Krall, A., Stanish, L., 2024. dataRetrieval: R packages for discovering and  
781 retrieving water data available from U.S. federal hydrologic web services.  
782 <https://doi.org/10.5066/P9X4L3GE>

783 DelVecchia, A.G., Shanafield, M., Zimmer, M.A., Busch, M.H., Krabbenhoft, C.A.,  
784 Stubbington, R., Kaiser, K.E., Burrows, R.M., Hosen, J., Datry, T., Kampf, S.K., Zipper,  
785 S.C., Fritz, K., Costigan, K., Allen, D.C., 2022. Reconceptualizing the hyporheic zone for  
786 nonperennial rivers and streams. *Freshwater Science* 000–000.  
787 <https://doi.org/10.1086/720071>

788 Dempsey, D., 2024. sensorstrings.

789 Dodds, W.K., Ratajczak, Z., Keen, R.M., Nippert, J.B., Grudzinski, B., Veach, A., Taylor, J.H.,  
790 Kuhl, A., 2023. Trajectories and state changes of a grassland stream and riparian zone  
791 after a decade of woody vegetation removal. *Ecological Applications* 33, e2830.  
792 <https://doi.org/10.1002/eap.2830>

793 Durand, M., 2020. TDPanalysis: Granier's Sap Flow Sensors (TDP) Analysis.

794 Durighetto, N., Noto, S., Tauro, F., Grimaldi, S., Botter, G., 2023. Integrating spatially-and  
795 temporally-heterogeneous data on river network dynamics using graph theory. *iScience*  
796 26. <https://doi.org/10.1016/j.isci.2023.107417>

797 Gama, J., 2015. thermocouple: Temperature Measurement with Thermocouples, RTD and IC  
798 Sensors.

799 Gambill, I., Zipper, S., Kirk, M.F., Seybold, E.C., 2024. Exploring drivers of groundwater  
800 recharge at Konza Prairie (Flint Hills region, Kansas, USA) using transfer function noise  
801 models (KGS Open-File Report 2024-6 No. 2024-6). Kansas Geological Survey,  
802 Lawrence KS.

803 Godsey, S., Wheeler, C., Zipper, S., 2024. AIMS SOP STIC Deployment and Maintenance.  
804 Godsey, S.E., Kirchner, J.W., 2014. Dynamic, discontinuous stream networks: hydrologically  
805 driven variations in active drainage density, flowing channels and stream order.  
806 *Hydrological Processes* 28, 5791–5803. <https://doi.org/10.1002/hyp.10310>

807 Hale, R.L., Godsey, S.E., 2019. Dynamic stream network intermittence explains emergent  
808 dissolved organic carbon chemostasis in headwaters. *Hydrological Processes* 33, 1926–  
809 1936. <https://doi.org/10.1002/hyp.13455>

810 Hale, R.L., Godsey, S.E., Dohman, J.M., Warix, S.R., 2024. Diel dissolved organic matter  
811 patterns reflect spatiotemporally varying sources and transformations along an  
812 intermittent stream. *Limnology and Oceanography*. <https://doi.org/10.1002/lno.12695>

813 Hall, C.A., Saia, S.M., Popp, A.L., Dogulu, N., Schymanski, S.J., Drost, N., van Emmerik, T.,  
814 Hut, R., 2022. A hydrologist’s guide to open science. *Hydrology and Earth System  
815 Sciences* 26, 647–664. <https://doi.org/10.5194/hess-26-647-2022>

816 Hatley, C.M., Armijo, B., Andrews, K., Anhold, C., Nippert, J.B., Kirk, M.F., 2023. Intermittent  
817 streamflow generation in a merokarst headwater catchment. *Environmental Science:  
818 Advances* 2, 115–131. <https://doi.org/10.1039/D2VA00191H>

819 Heffernan, J.B., 2008. Wetlands as an Alternative Stable State in Desert Streams. *Ecology* 89,  
820 1261–1271. <https://doi.org/10.1890/07-0915.1>

821 Jensen, C.K., McGuire, K.J., McLaughlin, D.L., Scott, D.T., 2019. Quantifying spatiotemporal  
822 variation in headwater stream length using flow intermittency sensors. *Environ Monit  
823 Assess* 191, 226. <https://doi.org/10.1007/s10661-019-7373-8>

824 Kaletová, T., Loures, L., Castanho, R.A., Aydin, E., Gama, J.T. da, Loures, A., Truchy, A.,  
825 2019. Relevance of Intermittent Rivers and Streams in Agricultural Landscape and Their  
826 Impact on Provided Ecosystem Services—A Mediterranean Case Study. *International  
827 Journal of Environmental Research and Public Health* 16, 2693.  
828 <https://doi.org/10.3390/ijerph16152693>

829 Kar, K.K., Roy, T., Zipper, S., Godsey, S.E., 2024. Nonlinear trends in signatures characterizing  
830 non-perennial US streams. *Journal of Hydrology* 635, 131131.  
831 <https://doi.org/10.1016/j.jhydrol.2024.131131>

832 Keen, R.M., Sadayappan, K., Jarecke, K.M., Li, L., Kirk, M.F., Sullivan, P.L., Nippert, J.B.,  
833 2024. Unexpected hydrologic response to ecosystem state change in tallgrass prairie.  
834 *Journal of Hydrology* 643, 131937. <https://doi.org/10.1016/j.jhydrol.2024.131937>

835 Kindred, T., 2022. Spatial Structure, Temporal Patterns, and Drivers of Stream Drying in the  
836 Gibson Jack Watershed, Bannock County, Idaho (M.S.). Idaho State University, United  
837 States -- Idaho.

838 Krabbenhoft, C.A., Allen, G.H., Lin, P., Godsey, S.E., Allen, D.C., Burrows, R.M., DelVecchia,  
839 A.G., Fritz, K.M., Shanafield, M., Burgin, A.J., Zimmer, M.A., Datry, T., Dodds, W.K.,  
840 Jones, C.N., Mims, M.C., Franklin, C., Hammond, J.C., Zipper, S., Ward, A.S., Costigan,  
841 K.H., Beck, H.E., Olden, J.D., 2022. Assessing placement bias of the global river gauge  
842 network. *Nat Sustain* 1–7. <https://doi.org/10.1038/s41893-022-00873-0>

843 Macpherson, G.L., 1996. Hydrogeology of thin limestones: the Konza Prairie Long-Term  
844 Ecological Research Site, Northeastern Kansas. *Journal of Hydrology* 186, 191–228.  
845 [https://doi.org/10.1016/S0022-1694\(96\)03029-6](https://doi.org/10.1016/S0022-1694(96)03029-6)

846 Malish, M.C., Gao, S., Allen, D.C., Neeson, T.M., 2024. Impacts of stream drying depend on  
847 stream network size and location of drying. *Ecological Applications* 34, e3015.  
848 <https://doi.org/10.1002/eap.3015>

849 Melton, F.S., Huntington, J., Grimm, R., Herring, J., Hall, M., Rollison, D., Erickson, T., Allen,  
850 R., Anderson, M., Fisher, J.B., Kilic, A., Senay, G.B., Volk, J., Hain, C., Johnson, L.,  
851 Ruhoff, A., Blankenau, P., Bromley, M., Carrara, W., Daudert, B., Doherty, C.,  
852 Dunkerly, C., Friedrichs, M., Guzman, A., Halverson, G., Hansen, J., Harding, J., Kang,  
853 Y., Ketchum, D., Minor, B., Morton, C., Ortega-Salazar, S., Ott, T., Ozdogan, M.,  
854 ReVelle, P.M., Schull, M., Wang, C., Yang, Y., Anderson, R.G., 2022. OpenET: Filling a  
855 Critical Data Gap in Water Management for the Western United States. *JAWRA Journal*  
856 *of the American Water Resources Association* 58, 971–994.  
857 <https://doi.org/10.1111/1752-1688.12956>

858 Messenger, M.L., Lehner, B., Cockburn, C., Lamouroux, N., Pella, H., Snelder, T., Tockner, K.,  
859 Trautmann, T., Watt, C., Datry, T., 2021. Global prevalence of non-perennial rivers and  
860 streams. *Nature* 594, 391–397. <https://doi.org/10.1038/s41586-021-03565-5>

861 Milford, C., Truong, B., 2024. Smart Rock [WWW Document]. URL  
862 <https://github.com/OPEnSLab-OSU/SmartRock?tab=readme-ov-file>

863 Newcomb, S.K., Godsey, S.E., 2023. Nonlinear Riparian Interactions Drive Changes in  
864 Headwater Streamflow. *Water Resources Research* 59, e2023WR034870.  
865 <https://doi.org/10.1029/2023WR034870>

866 Nippert, J.B., 2024. AWE01 Meteorological data from the konza prairie headquarters weather  
867 station. <https://doi.org/10.6073/pasta/910469efbf1f7e8d54c2b1ca864edec9>

868 Noorduijn, S.L., Shanafield, M., Trigg, M.A., Harrington, G.A., Cook, P.G., Peeters, L., 2014.  
869 Estimating seepage flux from ephemeral stream channels using surface water and  
870 groundwater level data. *Water Resources Research* 50, 1474–1489.  
871 <https://doi.org/10.1002/2012WR013424>

872 Paillex, A., Siebers, A.R., Ebi, C., Mesman, J., Robinson, C.T., 2020. High stream intermittency  
873 in an alpine fluvial network: Val Roseg, Switzerland. *Limnology and Oceanography* 65,  
874 557–568. <https://doi.org/10.1002/lno.11324>

875 Peterson, D.M., Flynn, S.M., Lanfear, R.S., Smith, C., Swenson, L.J., Belskis, A.M., Cook, S.C.,  
876 Wheeler, C.T., Wilhelm, J.F., Burgin, A.J., 2023. Team science: A syllabus for success  
877 on big projects. *Ecology and Evolution* 13, e10343. <https://doi.org/10.1002/ece3.10343>

878 Price, A.N., Jones, C.N., Hammond, J.C., Zimmer, M.A., Zipper, S.C., 2021. The Drying  
879 Regimes of Non-Perennial Rivers and Streams. *Geophysical Research Letters* 48,  
880 e2021GL093298. <https://doi.org/10.1029/2021GL093298>

881 Price, A.N., Zimmer, M.A., Bergstrom, A., Burgin, A.J., Seybold, E.C., Krabbenhoft, C.A.,  
882 Zipper, S., Busch, M.H., Dodds, W.K., Walters, A., Rogosch, J.S., Stubbington, R.,  
883 Walker, R.H., Stegen, J.C., Datry, T., Messenger, M., Olden, J., Godsey, S.E., Shanafield,  
884 M., Lytle, D., Burrows, R., Kaiser, K.E., Allen, G.H., Mims, M.C., Tonkin, J.D., Bogan,  
885 M., Hammond, J.C., Boersma, K., Myers-Pigg, A.N., DeVecchia, A., Allen, D., Yu, S.,  
886 Ward, A., 2024. Biogeochemical and community ecology responses to the wetting of  
887 non-perennial streams. *Nat Water* 2, 815–826. [https://doi.org/10.1038/s44221-024-](https://doi.org/10.1038/s44221-024-00298-3)  
888 00298-3

889 Read, J.S., Garner, B., Pellerin, B., Loken, L., 2015. sensorQC.  
890 Reinecke, R., Trautmann, T., Wagener, T., Schüler, K., 2022. The critical need to foster  
891 computational reproducibility. *Environ. Res. Lett.* 17, 041005.  
892 <https://doi.org/10.1088/1748-9326/ac5cf8>  
893 Sabathier, R., Singer, M.B., Stella, J.C., Roberts, D.A., Caylor, K.K., Jaeger, K.L., Olden, J.D.,  
894 2023. High resolution spatiotemporal patterns of flow at the landscape scale in montane  
895 non-perennial streams. *River Research and Applications* 39, 225–240.  
896 <https://doi.org/10.1002/rra.4076>  
897 Sadayappan, K., Keen, R., Jarecke, K.M., Moreno, V., Nippert, J.B., Kirk, M.F., Sullivan, P.L.,  
898 Li, L., 2023. Drier streams despite a wetter climate in woody-encroached grasslands.  
899 *Journal of Hydrology* 130388. <https://doi.org/10.1016/j.jhydrol.2023.130388>  
900 Sauquet, E., Shanafield, M., Hammond, J., Sefton, C., Leigh, C., Datry, T., 2021. Classification  
901 and trends in intermittent river flow regimes in Australia, northwestern Europe and USA:  
902 a global perspective. *Journal of Hydrology* 126170.  
903 <https://doi.org/10.1016/j.jhydrol.2021.126170>  
904 Shanafield, M., Bourke, S.A., Zimmer, M.A., Costigan, K.H., 2020a. An overview of the  
905 hydrology of non-perennial rivers and streams. *WIREs Water* 8, e1504.  
906 <https://doi.org/10.1002/wat2.1504>  
907 Shanafield, M., Cook, P.G., 2014. Transmission losses, infiltration and groundwater recharge  
908 through ephemeral and intermittent streambeds: A review of applied methods. *Journal of*  
909 *Hydrology* 511, 518–529. <https://doi.org/10.1016/j.jhydrol.2014.01.068>  
910 Shanafield, M., Gutiérrez-Jurado, K., White, N., Hatch, M., Keane, R., 2020b. Catchment-Scale  
911 Characterization of Intermittent Stream Infiltration; a Geophysics Approach. *Journal of*  
912 *Geophysical Research: Earth Surface* 125, e2019JF005330.  
913 <https://doi.org/10.1029/2019JF005330>  
914 Shaughnessy, A., Prener, C., Hasenmueller, E., 2018. driftR.  
915 <https://doi.org/10.5281/zenodo.1288819>  
916 Stagge, J.H., Rosenberg, D.E., Abdallah, A.M., Akbar, H., Attallah, N.A., James, R., 2019.  
917 Assessing data availability and research reproducibility in hydrology and water resources.  
918 *Scientific Data* 6, 190030. <https://doi.org/10.1038/sdata.2019.30>  
919 Stubbington, R., Acreman, M., Acuña, V., Boon, P.J., Boulton, A.J., England, J., Gilvear, D.,  
920 Sykes, T., Wood, P.J., 2020. Ecosystem services of temporary streams differ between wet  
921 and dry phases in regions with contrasting climates and economies. *People and Nature* 2,  
922 660–677. <https://doi.org/10.1002/pan3.10113>  
923 Sullivan, P.L., Zhang, C., Behm, M., Zhang, F., Macpherson, G.L., 2020. Toward a new  
924 conceptual model for groundwater flow in merokarst systems: Insights from multiple  
925 geophysical approaches. *Hydrological Processes* 34, 4697–4711.  
926 <https://doi.org/10.1002/hyp.13898>  
927 Swenson, L.J., Zipper, S., Peterson, D.M., Jones, C.N., Burgin, A.J., Seybold, E., Kirk, M.F.,  
928 Hatley, C., 2024. Changes in Water Age During Dry-Down of a Non-Perennial Stream.  
929 *Water Resources Research* 60, e2023WR034623.  
930 <https://doi.org/10.1029/2023WR034623>  
931 Trambly, Y., Rutkowska, A., Sauquet, E., Sefton, C., Laaha, G., Osuch, M., Albuquerque, T.,  
932 Alves, M.H., Banasik, K., Beaufort, A., Brocca, L., Camici, S., Csabai, Z., Dakhlaoui, H.,  
933 DeGirolamo, A.M., Dörflinger, G., Gallart, F., Gauster, T., Hanich, L., Kohnová, S.,  
934 Mediero, L., Plamen, N., Parry, S., Quintana-Seguí, P., Tzoraki, O., Datry, T., 2021.



935 Trends in flow intermittence for European rivers. *Hydrological Sciences Journal* 66, 37–  
936 49. <https://doi.org/10.1080/02626667.2020.1849708>

937 Vero, S.E., Macpherson, G.L., Sullivan, P.L., Brookfield, A.E., Nippert, J.B., Kirk, M.F., Datta,  
938 S., Kempton, P., 2018. Developing a Conceptual Framework of Landscape and  
939 Hydrology on Tallgrass Prairie: A Critical Zone Approach. *Vadose Zone Journal* 17, 0.  
940 <https://doi.org/10.2136/vzj2017.03.0069>

941 Volk, J.M., Huntington, J.L., Melton, F.S., Allen, R., Anderson, M., Fisher, J.B., Kilic, A.,  
942 Ruhoff, A., Senay, G.B., Minor, B., Morton, C., Ott, T., Johnson, L., Comini de Andrade,  
943 B., Carrara, W., Doherty, C.T., Dunkerly, C., Friedrichs, M., Guzman, A., Hain, C.,  
944 Halverson, G., Kang, Y., Knipper, K., Laipelt, L., Ortega-Salazar, S., Pearson, C.,  
945 Parrish, G.E.L., Purdy, A., ReVelle, P., Wang, T., Yang, Y., 2024. Assessing the  
946 accuracy of OpenET satellite-based evapotranspiration data to support water resource and  
947 land management applications. *Nat Water* 1–13. [https://doi.org/10.1038/s44221-023-](https://doi.org/10.1038/s44221-023-00181-7)  
948 [00181-7](https://doi.org/10.1038/s44221-023-00181-7)

949 Ward, A.S., Zarnetske, J.P., Baranov, V., Blaen, P.J., Brekenfeld, N., Chu, R., Derelle, R.,  
950 Drummond, J., Fleckenstein, J.H., Garayburu-Caruso, V., Graham, E., Hannah, D.,  
951 Harman, C.J., Herzog, S., Hixson, J., Knapp, J.L.A., Krause, S., Kurz, M.J.,  
952 Lewandowski, J., Li, A., Martí, E., Miller, M., Milner, A.M., Neil, K., Orsini, L.,  
953 Packman, A.I., Plont, S., Renteria, L., Roche, K., Royer, T., Schmadel, N.M., Segura, C.,  
954 Stegen, J., Toyoda, J., Wells, J., Wisnoski, N.I., Wondzell, S.M., 2019. Co-located  
955 contemporaneous mapping of morphological, hydrological, chemical, and biological  
956 conditions in a 5th-order mountain stream network, Oregon, USA. *Earth System Science*  
957 *Data* 11, 1567–1581. <https://doi.org/10.5194/essd-11-1567-2019>

958 Warix, S.R., Godsey, S.E., Flerchinger, G., Havens, S., Lohse, K.A., Bottenberg, H.C., Chu, X.,  
959 Hale, R.L., Seyfried, M., 2023. Evapotranspiration and groundwater inputs control the  
960 timing of diel cycling of stream drying during low-flow periods. *Front. Water* 5.  
961 <https://doi.org/10.3389/frwa.2023.1279838>

962 Warix, S.R., Godsey, S.E., Lohse, K.A., Hale, R.L., 2021. Influence of groundwater and  
963 topography on stream drying in semi-arid headwater streams. *Hydrological Processes* 35,  
964 e14185. <https://doi.org/10.1002/hyp.14185>

965 Wickham, H., Averick, M., Bryan, J., Chang, W., McGowan, L.D., François, R., Grolemund, G.,  
966 Hayes, A., Henry, L., Hester, J., Kuhn, M., Pedersen, T.L., Miller, E., Bache, S.M.,  
967 Müller, K., Ooms, J., Robinson, D., Seidel, D.P., Spinu, V., Takahashi, K., Vaughan, D.,  
968 Wilke, C., Woo, K., Yutani, H., 2019. Welcome to the Tidyverse. *Journal of Open*  
969 *Source Software* 4, 1686. <https://doi.org/10.21105/joss.01686>

970 Wilkinson, M.D., Dumontier, M., Aalbersberg, I.J., Appleton, G., Axton, M., Baak, A.,  
971 Blomberg, N., Boiten, J.-W., Santos, L.B. da S., Bourne, P.E., Bouwman, J., Brookes,  
972 A.J., Clark, T., Crosas, M., Dillo, I., Dumon, O., Edmunds, S., Evelo, C.T., Finkers, R.,  
973 Gonzalez-Beltran, A., Gray, A.J.G., Groth, P., Goble, C., Grethe, J.S., Heringa, J., Hoen,  
974 P.A.C. 't, Hooft, R., Kuhn, T., Kok, R., Kok, J., Lusher, S.J., Martone, M.E., Mons, A.,  
975 Packer, A.L., Persson, B., Rocca-Serra, P., Roos, M., Schaik, R. van, Sansone, S.-A.,  
976 Schultes, E., Sengstag, T., Slater, T., Strawn, G., Swertz, M.A., Thompson, M., Lei, J.  
977 van der, Mulligen, E. van, Velterop, J., Waagmeester, A., Wittenburg, P., Wolstencroft,  
978 K., Zhao, J., Mons, B., 2016. The FAIR Guiding Principles for scientific data  
979 management and stewardship. *Scientific Data* 3, 160018.  
980 <https://doi.org/10.1038/sdata.2016.18>

981 Zimmer, M.A., Burgin, A.J., Kaiser, K., Hosen, J., 2022. The unknown biogeochemical impacts  
982 of drying rivers and streams. *Nat Commun* 13, 7213. [https://doi.org/10.1038/s41467-022-](https://doi.org/10.1038/s41467-022-34903-4)  
983 34903-4

984 Zimmer, M.A., McGlynn, B.L., 2018. Lateral, Vertical, and Longitudinal Source Area  
985 Connectivity Drive Runoff and Carbon Export Across Watershed Scales. *Water*  
986 *Resources Research* 54, 1576–1598. <https://doi.org/10.1002/2017WR021718>

987 Zipper, S., Popescu, I., Compare, K., Zhang, C., Seybold, E.C., 2022. Alternative stable states  
988 and hydrological regime shifts in a large intermittent river. *Environ. Res. Lett.* 17,  
989 074005. <https://doi.org/10.1088/1748-9326/ac7539>

990 Zipper, S., Wheeler, C., Somerville, A., 2024. Kings Creek (Konza Prairie) Stream Temperature,  
991 Intermittency, and Conductivity Data (AIMS\_GP\_KNZ\_approach1\_STIC).

992 Zipper, S.C., Hammond, J.C., Shanafield, M., Zimmer, M., Datry, T., Jones, C.N., Kaiser, K.E.,  
993 Godsey, S.E., Burrows, R.M., Blaszcak, J.R., Busch, M.H., Price, A.N., Boersma, K.S.,  
994 Ward, A.S., Costigan, K., Allen, G.H., Krabbenhoft, C.A., Dodds, W.K., Mims, M.C.,  
995 Olden, J.D., Kampf, S.K., Burgin, A.J., Allen, D.C., 2021. Pervasive changes in stream  
996 intermittency across the United States. *Environ. Res. Lett.* 16, 084033.  
997 <https://doi.org/10.1088/1748-9326/ac14ec>

998 Zipper, S.C., Stack Whitney, K., Deines, J.M., Befus, K.M., Bhatia, U., Albers, S.J., Beecher, J.,  
999 Brelsford, C., Garcia, M., Gleeson, T., O'Donnell, F., Resnik, D., Schlager, E., 2019.  
1000 Balancing Open Science and Data Privacy in the Water Sciences. *Water Resources*  
1001 *Research* 55, 5202–5211. <https://doi.org/10.1029/2019WR025080>  
1002  
1003